

A 2D non linear method for travel time tomography: application to Mt. Vesuvius active seismic data

ALDO ZOLLO ⁽¹⁾, RAFFAELLA DE MATTEIS ⁽²⁾, LUCA D'AURIA ⁽¹⁾ and JEAN VIRIEUX ⁽³⁾

⁽¹⁾ *Dipartimento di Scienze Fisiche, Università di Napoli "Federico II", Napoli, Italy*

⁽²⁾ *Università degli Studi del Sannio, Benevento, Italy*

⁽³⁾ *UNSA-CNRS, UMR Geosciences Azur, Valbonne, France*

Abstract - We developed a non linear 2D tomographic method to interpret the first arrival times from the Mt. Vesuvius active seismic experiments. The use of a non-linear technique is justified by the lack of a refined reference model of the volcano and the weak data redundancy. The method is based on a spectral representation of the velocity field while the forward problem (travel time and ray computation) is solved using the asymptotic approximation for the wave equation solution. The velocity field is represented by the sum of polynomial and wavenumber spectral Fourier decomposed functions which account for the long wavelength velocity variations and short wavelength anomalies. In this case the ray vector equation is resolved locally by setting the initial conditions for ray position and parameter. We provide the iterative analytic expression for computing ray coordinates in a heterogeneous elastic 2D medium. The inverse method is based on a global/local optimization technique (Genetic Algorithm and Downhill Simplex) which explores the whole parameter space *i.e.* the coefficients of the polynomial and spectral Fourier functions. This spectral approach turns to be very efficient for applications to seismic tomography problems where the medium spectral content and the minimum resolved wavelength are generally unknown. In fact, a medium description through a Fourier series enables one to estimate by arrival time data inversion both the medium properties and the minimum resolvable wavelength in the tomographic study. The method was tested numerically simulating two canonical acquisition geometries and was then applied to a subset of data collected during the active seismic experiments performed in the Mt. Vesuvius area.

1 Introduction

In recent years, first arrival time tomography has become a rather standard tool to investigate the smooth velocity variation in complex geological environments. In particular it has been successfully applied to retrieve images of the shallow and deep structure of volcanoes where the medium complexity is related to the presence of densely fractured, fluid percolated lavas forming the volcano

edifice and/or of melting reservoir at depth. The input data sets for such studies are first P and S arrival times from active source (on land borehole explosions and offshore airgun shots) and/or microearthquake seismic recordings acquired in varied 2D and 3D source and receiver geometries. The joint use of active and passive sources in local seismic tomography studies proved very efficient since it minimizes the usual complications with local earthquake tomography which originate from the natural trade-off among the unknown source and medium parameters.

Different volcano images were obtained using local earthquake data (Kilauea volcano in Hawaii, Thurber, 1984; Campi Flegrei in Italy, Aster and Meyer, 1998; Mt. St. Helens in U.S.A., Lees and Crosson, 1989; Redoubt volcano in Alaska, Benz and Smith, 1984). In these studies anomalously low-velocity zones were detected with a spatial resolution about 5000-10000 m, and interpreted as magma reservoirs at depth. High resolution, active source seismic experiment (Medicine Lake in California, Evans and Zucca, 1988; Jasper seamount in California, Hammer *et al.*, 1994; Mt. Vesuvius in Southern Italy, Zollo *et al.*, 1996) also proved a powerful method to investigate volcano structures.

The tomography methods which are generally applied to the investigation of volcanic structures are based on approximate techniques for ray-tracing and travel time computation and/or iterative, linearized inversion schemes (Thurber, 1983; Eberhart-Phillips, 1986). This approach requires a rather well defined initial model for inversion and allows only for small velocity perturbations (few percent). Both these conditions are rarely verified in strongly heterogeneous media like volcanoes are expected to be.

In this paper we developed a non-linear tomographic method based on the exact first arrival ray tracing and travel time computation in a spectral decomposed medium. The velocity field $v(x, z)$ is represented by the sum of a polynomial and wavenumber spectral decomposed functions which account for the long wavelength velocity variations and short wavelength anomalies as proposed by Gjevik (1974). Since the minimum resolvable wavelength of the velocity field is generally not known *a priori*, the medium description by its wavelength components helps to detect the minimum wavelength limit of the tomographic study. A similar approach was recently used by Hammer *et al.* (1994). The method was applied to data collected during the 1994 and 1996 active seismic campaigns performed in the Mt. Vesuvius volcanic area (Gasparini *et al.*, 1998).

2 Non linear 2D arrival time inversion

We developed a non linear 2D inverse method to interpret the first arrival times from the Mt. Vesuvius active seismic experiments. Actually most strongly non-linear geophysical problems are investigated by global or mixed global/local optimization methods (Sen and Stoffa, 1997; Snieder, 1998). These overcome the difficulty of designing a reliable reference model of the complex volcano structure, by the weak data redundancy and the expected strong velocity heterogeneity,

typically encountered in linear/linearized inverse approaches. The method is based on a spectral representation of the velocity field while the forward problem (travel time and ray computation) is solved by using the asymptotic approximation for the wave equation solution.

We assume that the 2D velocity field $v(x, z)$ can be represented by the contribution of 1D and 2D terms

$$v(x, z) = v_L + v_H. \tag{1}$$

The term v_L :

$$v_L = \sum_{i=0}^P \sum_{j=0}^i p_{ij} x^i z^j$$

describes the long wavelength velocity variation in x, z directions (for instance, velocity gradients), where P is the order of the polynomial expansion and p_{ij} the related coefficients.

The term v_H

$$v_H = \sum_{m=1}^{M+1} \sum_{n=1}^{N+1} A_{mn} e^{i(mK_x x + nK_z z)} \quad x \quad z \tag{2}$$

represents the 2D velocity anomalies of the medium (short wavelengths), here described by a complex Fourier series expansion. In (2), A_{mn} are the complex coefficients of the Fourier series. Given the model dimensions L_x and L_z , the minimum wavenumbers K_x and K_z are defined as $2\pi/L_x$ and $2\pi/L_z$, respectively. The quantities Δx and Δz are the constant sampling intervals in the space domain which are dependent on the higher order numbers M and N considered in the Fourier series expansion ($\Delta x = L_x/M$; $\Delta z = L_z/N$).

The parametrization of the 2D medium velocity field through the function (1) provides an efficient and accurate way to compute analytically the space derivatives of the velocity field. Furthermore it has the advantage of explicitly describing the medium heterogeneities in terms of their wavenumber spectrum parameters.

The non linear inverse technique we used is based on the exhaustive search in the model parameter space for the minimum of a cost function, whose fast computation quests for a very efficient solution of the forward problem, *i.e.* the travel time computation in a 2D heterogeneous medium. Using the eq. (1), the vector equation for ray path in a heterogeneous 2D medium can be solved locally applying an analytical expression for the ray quantities (Appendix). A new ray position can be deduced from the previous one assuming locally a constant gradient of the square of the slowness (formulae (A.12) and (A.13) with a stepping parameter related to the arc length by $ds = v^{-1} dt$ (Červený, 1987; Virieux, 1988).

The inverse method is based on the exhaustive search in the model parameter space of the L_2 norm, assessing the distance between the observed and computed first P arrival times. The exploration of the model parameter space is performed

through a technique which employs at consecutive steps the Genetic Algorithm (GA) (Goldberg, 1989; Whitley, 1994) and the Downhill Simplex (DHS) (Press *et al.*, 1986) optimization methods. Both methods need only the cost function evaluation and not its derivatives.

In seismic tomography problems the model parameter resolution is strongly related to the minimum resolvable medium wavelength, which is generally unknown *a priori* and makes the choice of medium gridding extremely constraining. The adopted inversion strategy consists of performing several inversion cycles at increasing resolution degree. This can be naturally realized through the chosen model description by increasing at each step the order of the polynomial/Fourier series considered for the medium description. Firstly, the best-fit low order ($p, q < 3$) polynomial coefficients are found, which constrain the large wavelength variation of the medium (gradient, dipping layers). Secondly, the best fit coefficients of the Fourier series are searched by adding at each new cycle a coefficient in order to consider shorter wavelengths. The inversion process is stopped when the addition of a new parameter does not significantly improve the solution variance. The method does not require a reference model at the early inversion stage, as for the perturbative linearized technique. In order to speed up the search for the best fit solution at each inversion step the search is restricted within an arbitrary interval around the best fit coefficient values obtained in the previous step. At the end of the inversion process we obtain the minimum norm parameters and the minimum resolvable wavelength according to the adopted medium description.

Methods for resolution analysis have been mostly developed for linear and linearized inverse approaches and provide only local information, *i.e.* near the best fit model. These may not be obviously extrapolated to global/local optimization methods as the one we used here. For a qualitative estimate of resolution we adopted the analysis of ray density tensor as proposed by Kissling (1988). We call areal ray coverage the isotropic component and angular coverage its ellipticity. Although the ray density tensor has been developed for linear inverse methods, synthetic examples (see the next section) show that it represents a satisfying indicator of the spatial resolution in non-linear tomography. The best suited methods for complete resolution analysis are still a matter of the ongoing research (Zhang and Toksoz, 1998; Snieder, 1998).

3 Synthetic examples

The inversion method has been tested numerically simulating two canonical acquisition geometries: the cross-hole and global offset acquisition lay-outs.

In the cross-hole test the sources and receivers are located in two vertical parallel boreholes. An additional array of receivers is located at the model surface (Figure 1a). The synthetic P -velocity field shows a centered gaussian-like anomaly with a peak velocity 30% larger than the background value ($v_p = 3000$ m/s). The estimated model is compared to the synthetic one in Figure 1a. The global shape of the anomaly and the background velocity value are well recovered. The shape

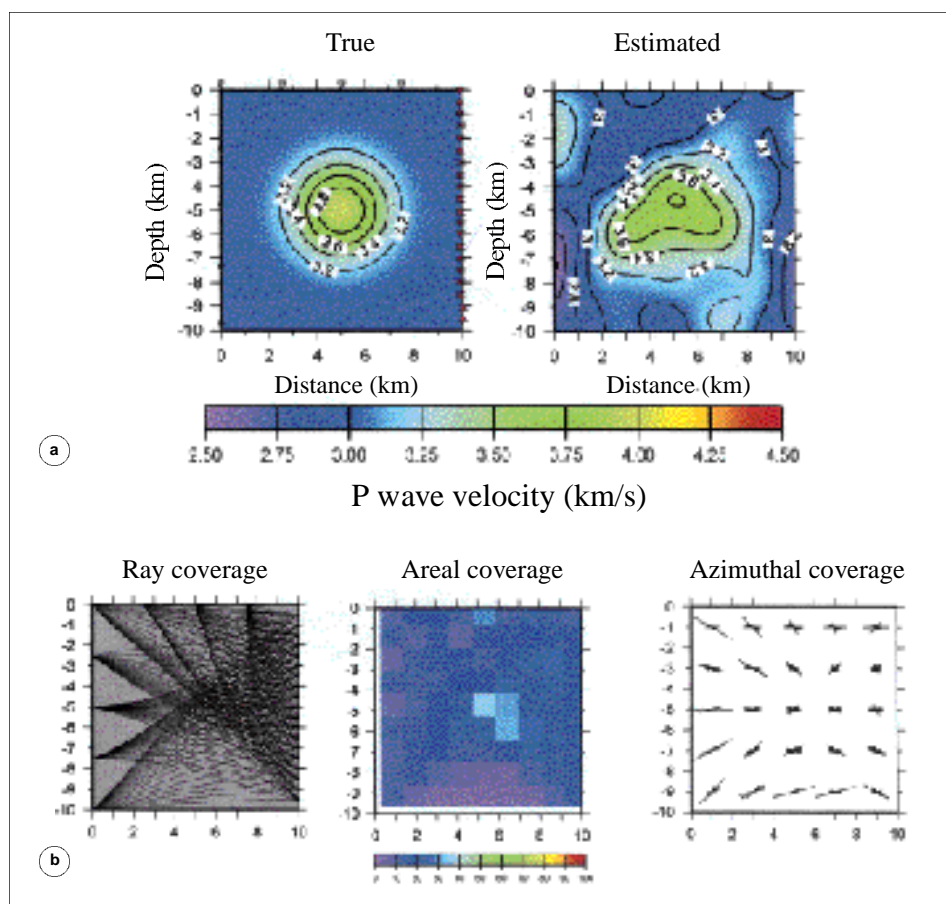


Figure 1a,b Synthetic test of the non linear inverse method using a typical cross-hole acquisition lay-out. (a) Source and receiver configuration and ray paths. Synthetic *versus* estimated 2D velocity model. (b) Model resolution. Ray, areal and angular coverage maps.

distortion of the retrieved anomaly is clearly related to the non uniform sampling of rays, areal and azimuthal coverages (Figure 1b). Residuals for the best fit model range between -0.02 s and 0.02 s. The final model shows a minimum resolvable wavelength $\lambda_x^{\min} = \lambda_z^{\min} = 1400$ m.

The global offset test represents the typical source and receiver configuration of 2D active seismic experiments at Mt. Vesuvius. Shots and receivers are both located at the topography of the investigated model section (Figure 2a). The P -velocity field is described by a truncated cone-like anomaly (peak = 1000 m/s and radius = 3000 m) with center position in ($x = 15000$ m; $z = 4000$ m) summed to a

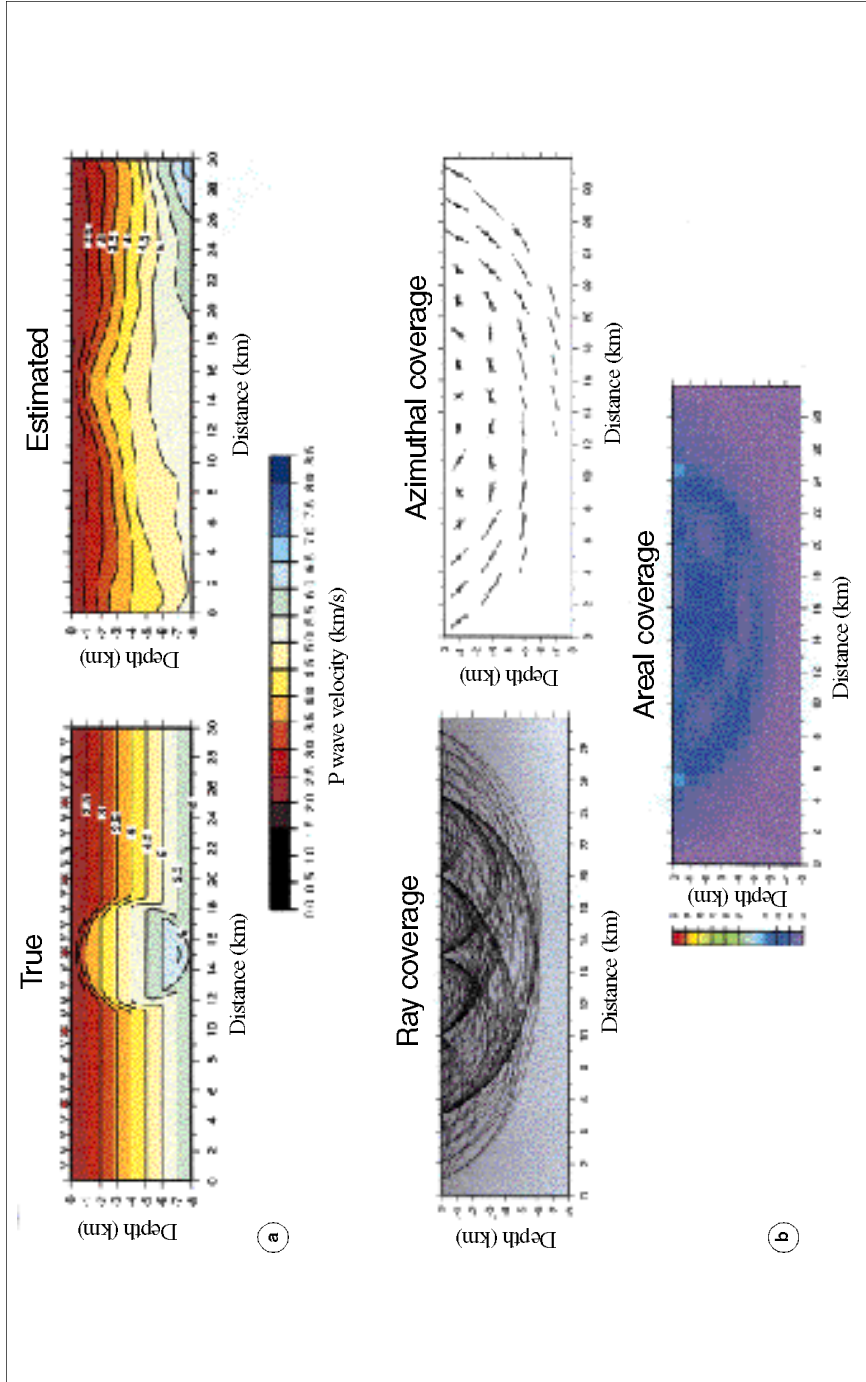


Figure 2a,b Synthetic test of the non linear inverse method using a typical global offset acquisition lay-out. (a) Source and receiver configuration and ray paths. Synthetic versus estimated 2D velocity model. (b) Model resolution. Ray, areal and azimuthal coverage maps.

vertical gradient velocity variation ($v(z) = (2000 + 500 z)$ m/s). The comparison between the synthetic and estimated models shows that the model is well constrained up to a depth of about 3000-4000 m which corresponds to the region of maximum ray, areal and azimuthal coverage. Resolution also degrades moving laterally from the section center (Figure 2b). Residuals for the best fit model range between -0.03 s and 0.03 s. The final model has different minimum resolvable wavelengths for x and z directions: $\lambda_x^{\min} = 1700$ m and $\lambda_z^{\min} = 900$ m.

4 Application to Mt. Vesuvius active seismic data

Two active seismic experiments were performed in the Mt. Vesuvius area in 1994 and 1996. Seismic sources were provided by 17 shots produced by 250 to 800 kg of seismic gel housed in 50 m deep boreholes. Shots and receivers were deployed along five 25 to 40 km profiles (A, B, C, D, Profile 94 in Figure 3). Profile 94 was performed in 1994 using 80 three-component seismographs which recorded three shots. Profiles A, B, C and D were carried out in 1996. During this campaign, 140 digital seismographs were deployed in the field. Each of them was equipped with 3C sensors having a natural frequency ranging between 2 and 4 Hz. The acquisition lay-out was planned according to a multi-2D source and receiver configuration (Figure 3). For each profile the shots have been recorded along the in-profile direction and the quasi-orthogonal one (*e.g.*, shot A1 was recorded simultaneously along the profiles A and C). This guarantees an optimal 2D and 3D coverage of the volcano although it is not a real 3D experiment. The station spacing was about 250 m on the volcano edifice and about 500 m outside. Seismic records were acquired at a sampling rate of 200 Hz. Further details on the experiments can be found in Gasparini *et al.* (1998).

An example of recorded common source section is shown in Figure 4. Clear first arrivals were detected as far as 25 000-30 000 m. Hand-picking of first arrival times was performed on unfiltered and filtered Common Source seismic sections. Traces were arranged as a function of the offset in order to improve the phase identification by waveform correlation.

Instead of a single reading with a weighting factor, a time window (t_1, t_2) was selected, bracketing the presumed first arrival time on each seismogram. t_1 is the observed phase arrival time. t_2 , larger than t_1 , is a measured time, whose distance from which t_1 expresses the uncertainty on the first arrival time picking (t_1). The width of the window (t_1, t_2) is related to the classical weighting factor, *i.e.* poor data quality is associated with a wide (t_1, t_2) window.

In addition, for large offsets and noisy records a single time reading can be performed. This time is associated to the first prominent amplitude arrival detected on the seismic records, not necessarily being the first P arrival. This time reading is useful in an approach based on global/local model parameter exploration since it provides a constrain *a posteriori* during the inversion procedure (*e.g.*, accepted models must provide theoretical first arrival times smaller than the measured t_2). It is not used for the misfit function calculation.

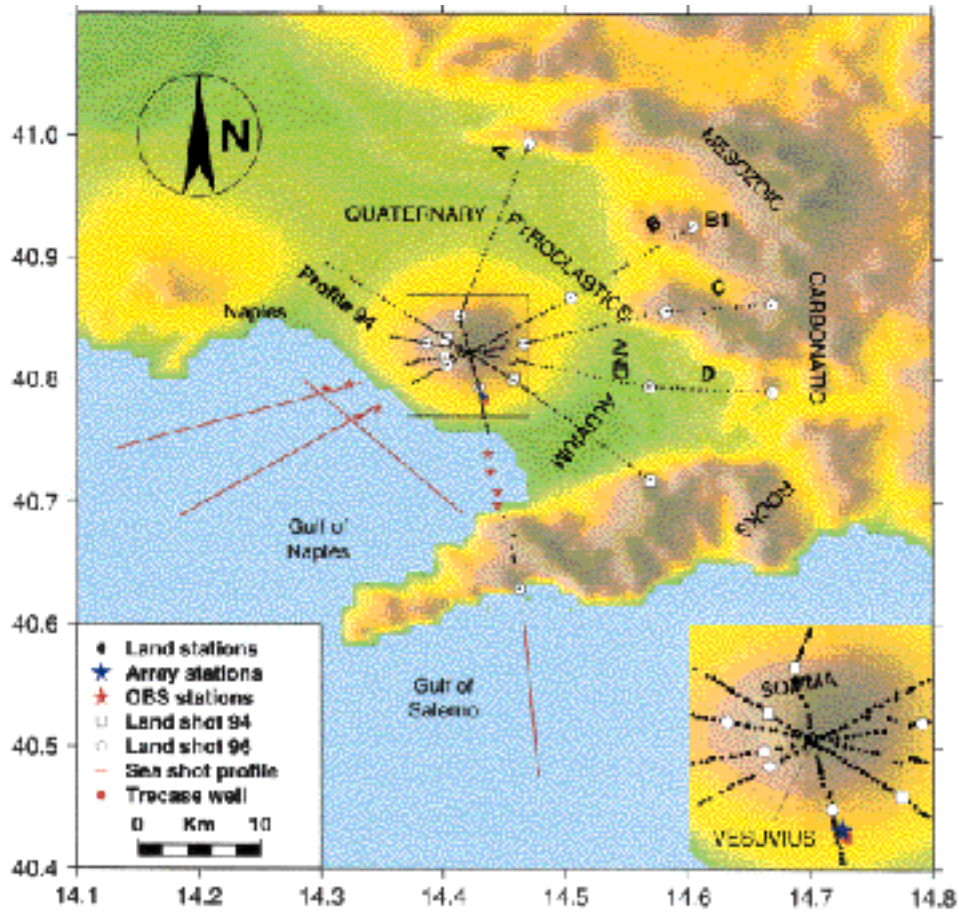


Figure 3 Map of the investigated area with active seismic profiles and the acquisition lay-out.

In this paper we analyzed data from the shot gathers along profile A. The travel time curves for shots along this profile are shown in Figure 5. The travel time curves show a significant change in the slope at offsets of 2-5 km. This is related to the arrival of a head-wave produced at the discontinuity between the volcanic/alluvial sediments and the Mesozoic limestones which is the prominent lithological transition at shallow depths (< 3000 m) underneath the Campanian Plain and the volcanic complex.

The 2D P -velocity model along profile A obtained using the spectral technique is displayed in Figure 6. A number of coefficients equal (17×9) was needed to represent the model: The smallest sampled wavelength is $x^{\min} = 1700$ m and $z^{\min} = 700$ m for the x and z directions respectively and the misfit between the observed and calculated models is 0.06 s.

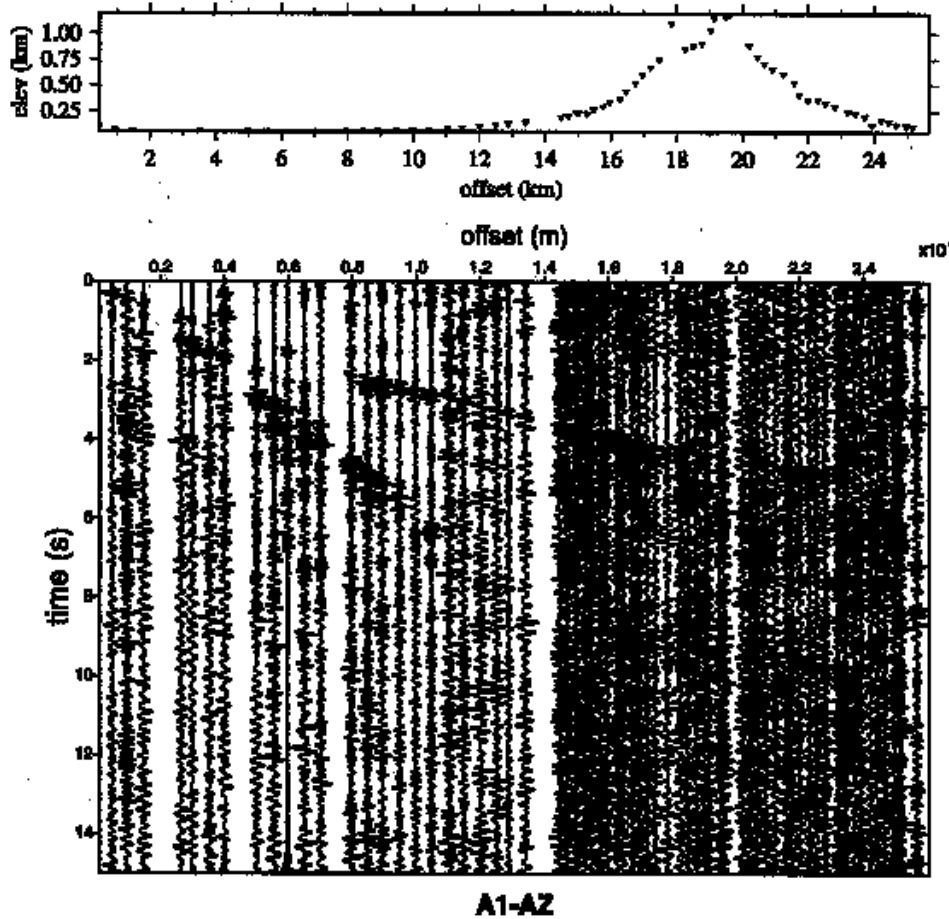


Figure 4 Example of a recorded seismic section along the profile A for the shot A1.

As expected for a “global offset” acquisition lay-out the resolution is higher in the vertical rather than in the horizontal direction. Comparing the azimuthal, areal and ray coverage maps (Figure 7) we conclude that the parameter resolution is higher in the middle part of the explored section and progressively diminishes moving outward. It also generally decreases with depth. The maximum resolvable depth is around 3000-4000 m.

The inferred P -velocity shows a high variability in the shallow volcanic structure, with values ranging from 1500 m/s to 6000 m/s. A very sharp velocity increase (from 3000-4000 m/s to 6000 m/s) is observed in the 2D image at depths ranging from a few hundreds meters to 2000-3000 m. Another prominent feature of the tomographic images is a relatively high velocity region ($v_p = 3500-4500$ m/s) located 1000-1500 m underneath the summit caldera of the volcano.

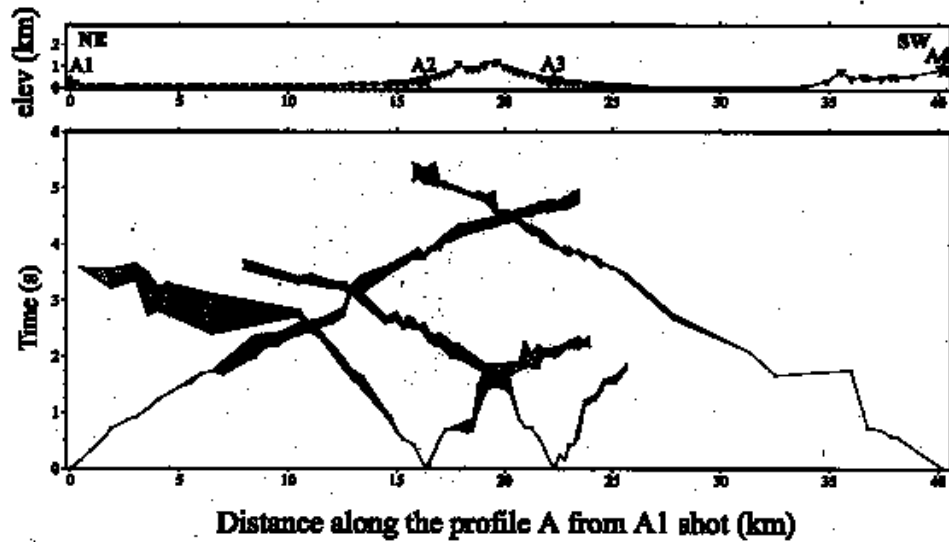


Figure 5 First P arrival time curves for shots along the profile A. The t_1 and t_2 time windows are displayed as a function of the distance from the shot.

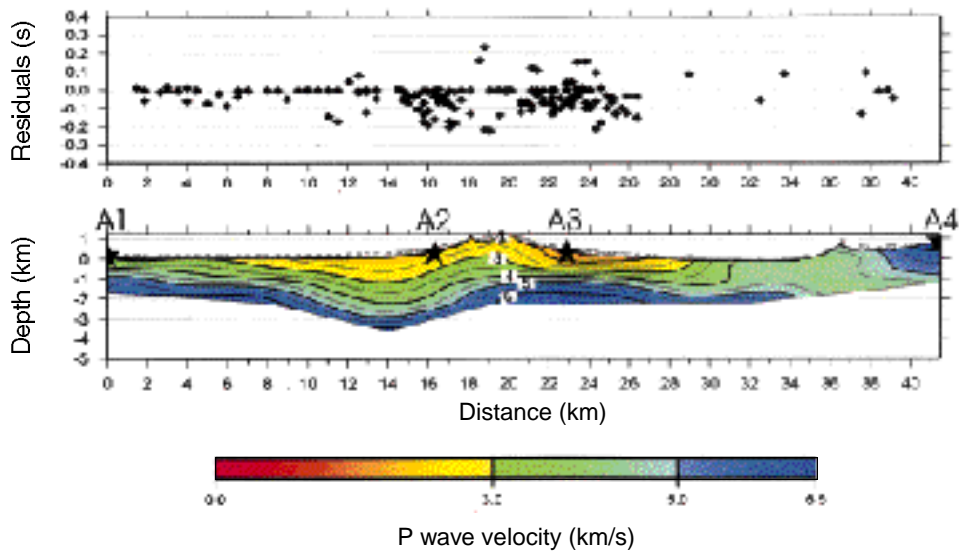


Figure 6 2D P -velocity model, relative to the section spanned by the profile A of the 1996 experiment, as inferred in this study from the non linear inversion of first arrival times.

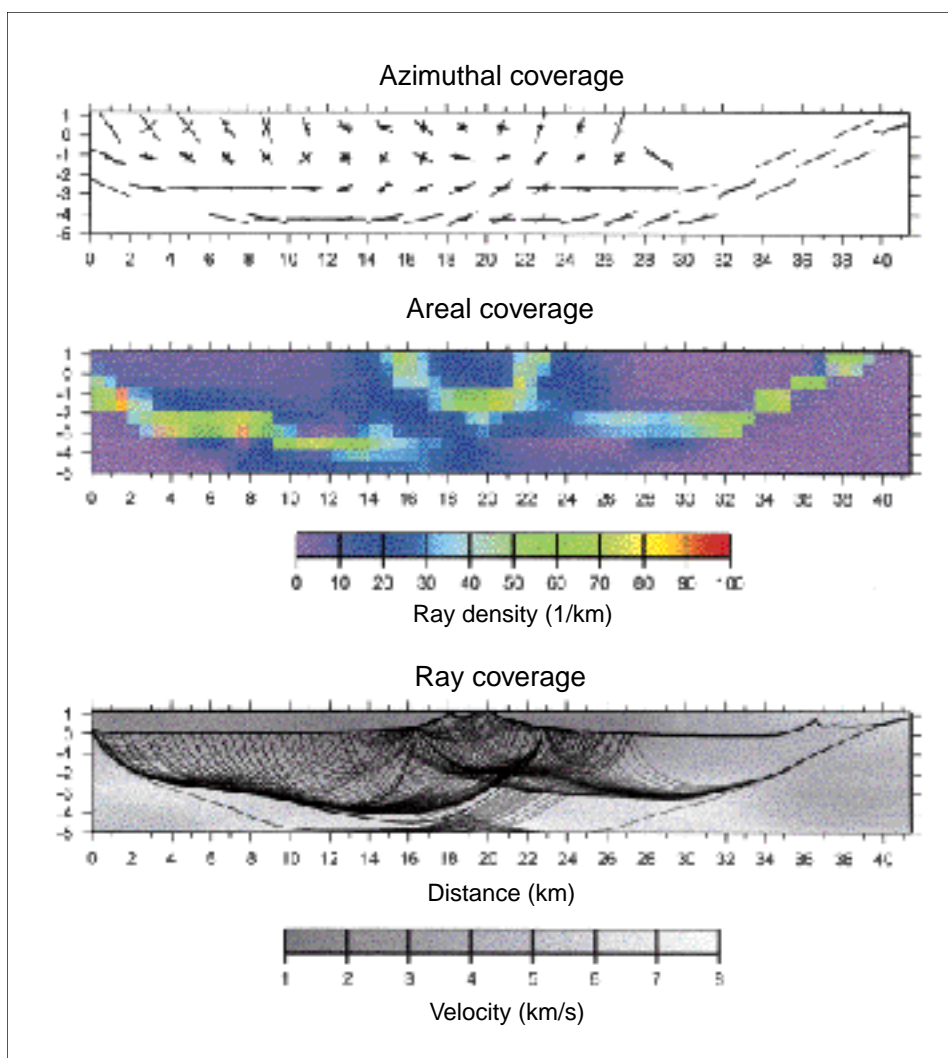


Figure 7 Model resolution. Ray, areal and azimuthal coverage maps for model section A.

5 Discussion and conclusions

We have applied a newly developed non linear inverse method which uses a spectral description of the propagation medium and an exact ray-tracing technique. Our synthetic simulations showed that the method is very efficient in the retrieval of velocity images of strongly heterogeneous structures such as volcanoes

provided that sources and receivers are adequately distributed around the target volume.

In tomographic problems the minimum velocity wavelength resolved by data is generally unknown *a priori*, which makes the choice of medium gridding subjective and critical. The proposed medium parametrization (Fourier decomposition) and the inversion strategy (moving from large to small wavelength model components) suggest a different approach to investigate the minimum wavelength resolved by data.

The latter is generally variable along the tomographic image and our method provides only an estimate of the wavelength associated with the retrieved highest degree coefficients which is an average value of the resolved wavelength on the whole image.

The exhaustive search for the cost function minimum is performed by coupling the Genetic and Downhill Simplex algorithms which ensure a quite efficient and fast procedure for model space sampling.

The method has been applied to retrieve the 2D images of the shallow structure of Mt. Vesuvius by the inversion of first *P* arrival times recorded during two recent active seismic experiments in the area. The 2D image shows a sharp *P*-velocity increase at a depth range of 2000-3000 m depth b.s.l. underneath the volcano. This sharp velocity transition can be associated with the passage from the Plio-Pleistocene volcano-sedimentary to the Mesozoic limestone formation (Zollo *et al.*, 2000).

This conclusion is supported by the lithostratigraphy and the laboratory ultrasonic measurements from the Trecase well samples (Zamora *et al.*, 1994). It can be reasonably assumed that the *P*-velocity isoline at 5500 m/s marks the position of this discontinuity in the tomographic images.

The limestone top has an irregular shape and generally dips from the edges of the Campanian Plain toward the volcano. This trend is also consistent with the Bouguer anomalies pattern (Cassano and La Torre, 1987; Berrino *et al.*, 1998).

Interestingly, the analyzed velocity section shows an important depression in the morphology of the limestone top about 9000 m long and 1000 m deep extending North of Mt. Somma. It can be related to a graben-like structure.

The high velocity body overlaying the Mesozoic limestone underneath the summit caldera can be associated with a paleo-volcanic or a sub-volcanic (solidified dikes) structure. In fact the range of observed velocities ($v_p = 3500-4500$ m/s) is consistent with *in-situ* and laboratory measurements of solidified lavas (Bernard, 1999; Zamora *et al.*, 1994).

Acknowledgements

A. Herrero and P. Gasparini are acknowledged for the many useful discussions and suggestions on the non linear method and results' implications for the Mt. Vesuvius structure. We thank A. Morelli for helpful comments and revision of the manuscript. This work was funded by EU, contract No. ENV4-980698.

Appendix The ray path and travelttime equations.

Let us recall the vector equation for ray trajectory in a heterogeneous 2D medium

$$\frac{d}{dr} s(\mathbf{x}) \frac{d\mathbf{x}}{dr} = -s(\mathbf{x}) \mathbf{x} \quad (\text{A.1})$$

where $s(\mathbf{x}) = 1/v(\mathbf{x})$ is the slowness, v is given by eq. (1) and $\mathbf{x} = (x, z)$ is the ray vector expressed in its cartesian components. dr is curved elementary distance calculated along the ray path. It can be shown that eq. (A.1) can be split in two equations for $\mathbf{p} = (p_x, p_z)$, the ray parameter vector, and for \mathbf{x} (Virieux, 1996)

$$\frac{d\mathbf{p}}{dr} = -s(\mathbf{x}) \mathbf{p} \quad (\text{A.2})$$

$$\frac{d\mathbf{x}}{dr} = v\mathbf{p} \quad (\text{A.3})$$

According to Virieux *et al.* (1988) we introduce the variable d , defined by the equation

$$s \, d = dr.$$

The variable d depends on wave velocity and is therefore a function of the ray position. By changing the variable in eqs. (A.2) and (A.3), these can be rewritten as a function of

$$\frac{d\mathbf{p}}{d} = -s \, \mathbf{p} \quad s = \frac{1}{2} \frac{ds^2}{d} \quad (\text{A.4})$$

$$\frac{d\mathbf{x}}{d} = v \mathbf{p} \quad (\text{A.5})$$

The vector $\mathbf{x}(d) = (x(d), z(d))$ gives the ray coordinates along the travel path.

The differential eqs. (A.4) and (A.5) allow one to obtain the values of ray parameter and coordinates at a given point along the ray path knowing their values at a neighbouring, previous point along the same trajectory. Therefore, these equations are defined locally along the ray path and can be applied to trace rays through an iterative procedure moving from the source position to the receiver. In order to solve analytically eqs. (A.4) and (A.5) we compute the squared slowness

their initial values at point (x_0, z_0) and an arbitrary value of α . The travel time is given by

$$T = T_0 + s^2 + \alpha \cdot \mathbf{p}^2 + 1/3 \cdot \mathbf{p}^3. \quad (\text{A.11})$$

We can generalize these equations to obtain the following iterative formulae for obtaining the ray parameter and coordinates at any point (x_N, z_N)

$$x_N(\alpha) = \frac{1}{2} [x]_{x_{N-1}}^2 + p_{x_{N-1}} + x_{N-1} \quad (\text{A.12})$$

$$z_N(\alpha) = \frac{1}{2} [z]_{z_{N-1}}^2 + p_{z_{N-1}} + z_{N-1}$$

$$p_x^N = [x]_{x_{N-1}} + p_x^{N-1} \quad (\text{A.13})$$

$$p_z^N = [z]_{z_{N-1}} + p_z^{N-1}.$$

The travel time is computed through the expression

$$T_N = T_{N-1} + s_{N-1}^2 + \alpha \cdot p_{N-1}^2 + 1/3 (\frac{\partial}{\partial x} + \frac{\partial}{\partial z})_{N-1}^3. \quad (\text{A.14})$$

The parameter α controls the sampling length along the ray path, which therefore depends on the ray position and on the local wave velocity. As a general rule, small values of α (typically $< 0.1 \text{ km}^2/\text{s}$) correspond to a fine sampling of the ray path (ray-path arc sampling length $l < 0.025 \text{ km}$ with a velocity around 4 km/s).

The code has been tested by comparing ray paths and travel times using eqs. (A.12), (A.13) and (A.14) and those computed analytically in 2D synthetic media obtained by summing up a gaussian-like symmetric anomaly to a vertical gradient velocity function.

REFERENCES

- ASTER, R. and R.P. MEYER (1988): Three-dimensional velocity structure and hypocenter distribution in the Campi Flegrei caldera, Italy, *Tectonophysics*, **149**, 195-218.
- BENZ, H.M. and R.B. SMITH (1984): Simultaneous inversion for lateral velocity variations and hypocenters in the yellowstone region using earthquake and refraction data, *J. Geophys. Res.*, **89**, 1208-1220.
- BERNARD, M.-L. (1999): Étude expérimentale des propriétés physiques des roches pyroclastiques de la Montagne Pelee, *Ph.D. Thesis*, Université de Paris VII, France.
- BERRINO, G., G. CORRADO and U. RICCARDI (1998): Sea gravity data in the Gulf of Naples: a contribution to delineating the structural pattern of the vesuvian area, *J. Geophys. Res.*, **82**, 139-150.
- CASSANO, E. and P. LA TORRE (1987): Geophysics, in *Somma-Vesuvius* edited by R. SANTACROCE, CNR, 175-196.
- ČERVENÝ, V. (1987): Ray tracing algorithms in three dimensional laterally varying layered structures, in *Tomography in Seismology and Exploration Seismics*, edited by G. NOLET (D. Réidel, Norwell, Ma), pp. 530.

- EBERHART-PHILLIPS, D. (1986): Three-dimensional velocity structure in Northern California coast ranges from inversion of local earthquakes, *Bull. Seismol.Soc. Am.*, **76**, 1025-1052.
- EVANS, J.R. and J.J. ZUCCA (1988): Active high resolution seismic tomography of compressional wave velocity and attenuation at medicine lake volcano, Northern California cascade range, *J.Geophys. Res.*, **93**, 15016-15036.
- GASPARINI, P. and TOMOVES WORKING GROUP (1998): Tomoves: a project of seismic investigation of Mt. Vesuvius, *EOS Trans. AGU*, **79** (19), 229-231.
- GJEVIK, B. (1974): Ray tracing for seismic surface waves, *Geophys.J.R. Astron.Soc.*, **29**, 29-39.
- GOLDBERG, X. (1989): *Genetic Algorithm in Search, Optimization and Machine Learning* (Addison-Wesley Pub. Co.), pp.432.
- HAMMER, P.T.C., L.M. DORMAN, J.A. HILDEBRAND and M.D. CORNUELLE (1994): Jasper seamount structure: seafloor seismic refraction tomography, *J.Geophys.Res.*, **99**, 6731-6752.
- KISSLING, E. (1988): Geotomography with local earthquake data, *Rev. Geophys.*, **26**, 659-698.
- LEES, J.M. and R.S. CROSSON (1989): Tomographic inversion for three dimensional velocity structure at mount St. Helens using earthquake data, *J. Geophys. Res.*, **94**, 5716-5728.
- PRESS, W.H., B.P. FLANNERY, S.A. TEUKOLSKY and W.T. VETTERLING (1986): *Numerical Recipes* (Cambridge University Press, Cambridge), pp. 818.
- SEN, M.K. and P.L. STOFFA (1997): *Global Optimization Methods in Geophysical Inversion* (Elsevier Science), pp.280.
- SNIEDER, R. (1983): The rule of non-linearity in inverse problems, *Inverse Problems*, **14**, 3.
- THURBER, C.H. (1983): Earthquake locations and three dimensional crustal structure in the coyote lake area, central California, *J. Geophys. Res.*, **88**, 8226-8236.
- THURBER, C.H. (1984): Seismic detection of the summit magma complex of Kilauea volcano, Hawaii, *Science*, **223**, 165-167.
- VIRIEUX, J. (1996): Seismic ray tracing, in *Seismic Modelling of Earth Structure*, edited by E. BOSCHI, G. EKSTRÖM and A. MORELLI (ING, Rome), pp. 582.
- VIRIEUX, J., V. FARRA and R. MADARIAGA (1988): Ray tracing in laterally heterogeneous media for earthquake location, *J. Geophys.Res.*, **93**, 6585-6599.
- WHITLEY, D. (1994): *A Genetic Algorithm Tutorial* (Samizdat Press), pp. 37.
- ZAMORA, M., G. SARTORIS and W. CHELINI (1994): Laboratory measurements of ultrasonic wave velocities in rocks from the Campi Flegrei volcanic system and their relation to other field data, *J. Geophys. Res.*, **99**, 13553-13561.
- ZHANG, J. and M.N. TOKSOZ (1998): Nonlinear refraction travelttime tomography, *Geophysics*, **63** (5), 1726-1737.
- ZOLLO, A., P. GASPARINI, J. VIRIEUX, H. LE MEUR, G. DE NATALE, G. BIELLA, E. BOSCHI, P. CAPUANO, R. DE FRANCO, P. DELL'AVERSANA, R. DE MATTEIS, I. GUERRA, G. IANNACCONE, L. MIRABILE and G. VILARDO (1996): Seismic evidence for a low velocity zone in the upper crust beneath Mount Vesuvius, *Science*, **274**, 592-594.
- ZOLLO, A., L. D'AURIA, R. DE MATTEIS, A. HERRERO and P. GASPARINI (2000): Bayesian estimation of 2D *P*-velocity models from active seismic arrival time data: imaging of the shallow structure of Mt. Vesuvius (Southern Italy), *J.Geophys. Res.* (submitted).